Low-PAPR DFRC MIMO-OFDM Waveform Design for Integrated Sensing and Communications

Xiaoyan Hu, Christos Masouros, Fan Liu and Ronald Nissel
Department of Electronic and Electrical Engineering, University College London, London, UK
Department of Electical and Electronic Engineering, Southern University of Science and Technology, Shenzhen, China
Huawei Technologies, Gothenburg, Sweden
Email:{xiaoyan.hu, c.masouros}@ucl.ac.uk, liuf6@sustech.cn, ronald.nissel@huawei.com

***Abstract*—In this paper, we explore a multiple-input multiple-output (MIMO) system with orthogonal frequency division multiplexing (OFDM) transmissions and study the low peak-to-average power ratio (PAPR) MIMO-OFDM waveform design for integrated sensing and communications (ISAC). This is done by utilizing a weighted objective function on both communication and radar performance metrics under power and PAPR constraints. The formulated optimization problem can be equivalently transformed into several sub-problems which can be parallelly solved by the semi-definite relaxation (SDR) method and the optimal rank-1 solution can be obtained in general. The feasibility, effectiveness, and flexibility of the proposed low-PAPR MIMO-OFDM waveform design method are demonstrated by a range of simulations on communication sum rate, symbol error rate as well as radar beampattern and detection probability.**

I. Introduction

The critical shortage of spectrum resources has driven the spectrum reuse between radar and communications, which has been regarded as a promising way for achieving a win-win policy for both sides. As a step further, with sharing one set of hardware equipment and signal processing frameworks for communications and radar, dual-functional radar-communication (DFRC) design provides a cost-efficient solution for achieving integrated sensing and communications (ISAC), which have drawn great attention from both academia and industry [1–4]. DFRC systems aim at fulfilling wireless communications and radar detections simultaneously through designing a single transmitted waveform. Recently, more attention is focused on *DFRC systems with joint DFRC waveform design* [5, 6] to guarantee both sensing and communication performance, which is not limited by any existing radar or communication waveforms and is promising to achieve scalable performance trade-off between the two functionalities.

As a key enabler for 4G and 5G wireless networks, the technique of orthogonal frequency division multiplexing (OFDM) is part of communication standards and has been studied extensively [7, 8]. Actually, OFDM has also recently been exploited for radar sensing [9–11]. The orthogonal property of OFDM waveform fulfilled by the discrete Fourier transform (DFT) and inverse DFT (IDFT) operations at transceivers can facilitate signal processing for both communications and radar sensing. Even though OFDM waveform is an excellent candidate for joint design of DFRC systems, one major disadvantage of OFDM waveform is high peak-to-average power ratio (PAPR) which should be effectively dealt with. Otherwise, high PAPR may cause non-linear distortion of the transmit signals and lead to radar/communication performance degradation considering the limited linear region of the low-cost power amplifiers [12, 13]. However, to the best of our knowledge, most of the DFRC OFDM systems in the state-of-the-art literature have not taken the PAPR constraints into consideration, especially for the joint design DFRC systems.

II. System Model

We consider a wideband DFRC MIMO-OFDM system, where a DFRC-BS equipped with a uniform linear array (ULA) of N_{t}-antenna transmits DFRC waveforms, aiming at serving K downlink single-antenna user equipment (UEs) and sensing M far-field targets simultaneously. Our objective is to effectively design the transmitted DFRC MIMO-OFDM waveform under transmit power and specific PAPR constraints, so as to obtain desirable low-PAPR DFRC MIMO-OFDM waveform achieving satisfactory performance tradeoff between communications and radar functionalities.

A. DFRC MIMO-OFDM Waveform Formulation

We assume that the wireless communication channels are with the memory of $U-1$, i.e., each has U effectively non-zero channel taps. In addition, the length of the effective data symbols in each block is N_{s} which need modulate N_{s} subcarriers for transmissions [7], and we denote the index of symbols/subcarriers as $n \in \mathcal{N}_{\mathrm{s}} = \{1, \cdots, N_{\mathrm{s}}\}$. In order to eliminate inter-symbol interference (ISI) of wideband multi-carrier transmissions, the standard OFDM technique of cyclic prefix (CP) is utilized [8]. The length of CP is denoted as N_{c} with $N_{\mathrm{c}} \geq U-1$, and thus the total number of time-domain samples per block is $N = N_{\mathrm{s}} + N_{\mathrm{c}}$. Without lose of generality, we use $N_{\mathrm{c}} = U-1$ in this paper.

1) Symbol Data and Preoding Model: Let

$$\mathbf{S} = [\mathbf{S}_1^{\mathrm{T}}, \cdots, \mathbf{S}_{N_{\mathrm{s}}}^{\mathrm{T}}]^{\mathrm{T}} \in \mathbb{C}^{N_{\mathrm{s}}K \times L} \tag{1}$$

represent the symbol data matrix for all UEs of $k \in \mathcal{K} = \{1, \cdots, K\}$ on N_{s} subcarriers, transmitted during a communication frame with length L.[1] Here, $\mathbf{S}_n = [\mathbf{s}_{n,1}, \cdots, \mathbf{s}_{n,K}]^{\mathrm{T}} \in \mathbb{C}^{K \times L}$ is the symbol matrix for all UEs on subcarrier $n \in \mathcal{N}_{\mathrm{s}}$ with $\mathbf{s}_{n,k} \in \mathbb{C}^{L \times 1}$ being the specific symbol vector for user k. In addition, $\mathbf{W} = \mathrm{diag}(\mathbf{W}_1, \cdots, \mathbf{W}_{N_{\mathrm{s}}}) \in \mathbb{C}^{N_{\mathrm{s}}N_{\mathrm{t}} \times N_{\mathrm{s}}K}$ is the compact precoding matrix for all UEs on all subcarriers where $\mathbf{W}_n = [\mathbf{w}_{n,1}, \cdots, \mathbf{w}_{n,K}] \in \mathbb{C}^{N_{\mathrm{t}} \times K}$ is the precoding matrix for all UEs on subcarrier $n \in \mathcal{N}_{\mathrm{s}}$ with $\mathbf{w}_{n,k} \in \mathbb{C}^{N_{\mathrm{t}} \times 1}$ being the specific precoding vector for user k.

[1] L is the length of the radar snapshot/communication frame, corresponding to the number of OFDM symbols in the time domain.

The transmit symbol data $\mathbf{S}$ is first precoded by $\mathbf{W}$ in the frequency domain and then converted to the time domain by IDFT operation before subcarrier modulations. We further use

$$\mathbf{X}_{\rm s} = \mathbf{W}\mathbf{S} = [\mathbf{X}_1^{\rm T}, \cdots, \mathbf{X}_{N_{\rm s}}^{\rm T}]^{\rm T} \in \mathbb{C}^{N_{\rm s}N_{\rm t}\times L} \tag{2}$$

to indicate the baseband precoded symbol matrix on all subcarriers before the IDFT processing where $\mathbf{X}_n = \mathbf{W}_n\mathbf{S}_n \in \mathbb{C}^{N_{\rm t}\times L}$ for $n \in \mathcal{N}_{\rm s}$. We denote $\mathbf{F}_{\rm s} \in \mathbb{C}^{N_{\rm s}\times N_{\rm s}}$ as the normalized DFT matrix for data transmissions with

$$F_{n,m}^{\rm s} = \frac{1}{\sqrt{N_{\rm s}}} e^{-\frac{j2\pi}{N_{\rm s}}(n-1)(m-1)} \tag{3}$$

being the (n,m)-th element of $\mathbf{F}_{\rm s}$ for $n, m \in \mathcal{N}_{\rm s}$. The IDFT processing at the transmitter of the DFRC-BS is operated by $(\mathbf{F}_{\rm s}^{\rm H} \otimes \mathbf{I}_{N_{\rm t}}) \in \mathbb{C}^{N_{\rm s}N_{\rm t}\times N_{\rm s}N_{\rm t}}$ considering the fact that the ULA array is equipped with $N_{\rm t}$ transmit antennas. Hence, the transmitted time-domain data signal waveform after IDFT can be further expressed as

$$\mathbf{G} \triangleq (\mathbf{F}_{\rm s}^{\rm H} \otimes \mathbf{I}_{N_{\rm t}})\mathbf{X}_{\rm s} = [\mathbf{G}_1^{\rm T}, \cdots, \mathbf{G}_{N_{\rm s}}^{\rm T}]^{\rm T} \in \mathbb{C}^{N_{\rm s}N_{\rm t}\times L}, \tag{4}$$

where $\mathbf{G}_n = (\mathbf{f}_{{\rm s},n}^{\rm H} \otimes \mathbf{I}_{N_{\rm t}})\mathbf{X}_{\rm s} \in \mathbb{C}^{N_{\rm t}\times L}$ is the transmitted DFRC MIMO-OFDM signal from $N_{\rm t}$ antennas on the n-th subcarrier with $\mathbf{f}_{{\rm s},n} \in \mathbb{C}^{N_{\rm s}\times 1}$ being the n-th column of $\mathbf{F}_{\rm s}$ corresponding to the (I)DFT operations on the n-th subcarrier.

2) DFRC MIMO-OFDM Waveform with CP: The next step is adding CP with size $N_{\rm c} = U - 1$, which is crucial for eliminating the ISI caused by multi-path frequency-selective fading. It is operated by repeating the last $N_{\rm c}$ symbols at the beginning of the original symbol sequence [14]. We denote

$$\mathbf{X}_{\rm c} = [\mathbf{X}_{N_{\rm s}-N_{\rm c}+1}^{\rm T}, \mathbf{X}_{N_{\rm s}-N_{\rm c}+2}^{\rm T}, \cdots, \mathbf{X}_{N_{\rm s}}^{\rm T}]^{\rm T} \in \mathbb{C}^{N_{\rm c}N_{\rm t}\times L}, \tag{5}$$

$$\mathbf{F}_{\rm c} = [\mathbf{f}_{{\rm s},N_{\rm s}-N_{\rm c}+1}, \mathbf{f}_{{\rm s},N_{\rm s}-N_{\rm c}+2}, \cdots, \mathbf{f}_{{\rm s},N_{\rm s}}] \in \mathbb{C}^{N_{\rm s}\times N_{\rm c}}, \tag{6}$$

and let $\dot{\mathbf{X}} = [\mathbf{X}_{\rm c}^{\rm T}, \mathbf{X}_{\rm s}^{\rm T}]^{\rm T} \in \mathbb{C}^{NN_{\rm t}\times L}$ and $\dot{\mathbf{F}} = [\mathbf{F}_{\rm c}, \mathbf{F}_{\rm s}] \in \mathbb{C}^{N_{\rm s}\times N}$, then the transmitted DFRC MIMO-OFDM waveform after adding CP can be expressed as

$$\begin{aligned}\dot{\mathbf{G}} &\triangleq (\dot{\mathbf{F}}^{\rm H} \otimes \mathbf{I}_{N_{\rm t}})\dot{\mathbf{X}} \in \mathbb{C}^{NN_{\rm t}\times L} \\ &= [\mathbf{G}_{N_{\rm s}-N_{\rm c}+1}^{\rm T}, \mathbf{G}_{N_{\rm s}-N_{\rm c}+2}^{\rm T}, \cdots, \mathbf{G}_{N_{\rm s}}^{\rm T}, \mathbf{G}_1^{\rm T}, \cdots, \mathbf{G}_{N_{\rm s}}^{\rm T}]^{\rm T},\end{aligned} \tag{7}$$

recalling that $N = N_{\rm c} + N_{\rm s}$. Through operating the IDFT and adding the CP at the transmitter side, the effects of ISI caused by frequency-selective fading can be eliminated after removing the CP and operating the DFT at the receiver side.

B. MIMO-OFDM Communication Model

1) Overall Downlink Channel and Received Signal: After adding the CP, the signal is then up-converted to the radio frequency (RF) domain through subcarrier modulations for transmission via $N_{\rm t}$ RF chains connected to $N_{\rm t}$ antennas. We denote $\widetilde{\mathbf{H}}_u = [\widetilde{\mathbf{h}}_{1,u}^{\rm T}, \cdots, \widetilde{\mathbf{h}}_{K,u}^{\rm T}]^{\rm T} \in \mathbb{C}^{K\times N_{\rm t}}$ as the channel matrix of the u-th tap for $u \in \mathcal{U} = \{0, \cdots, U-1\}$, where $\widetilde{\mathbf{h}}_{k,u} \in \mathbb{C}^{1\times N_{\rm t}} \sim \mathcal{CN}(0, \frac{1}{U}\mathbf{I}_{N_{\rm t}})$ is the corresponding channel vector for UE $k \in \mathcal{K}$ with independent identically distributed (i.i.d.) Rayleigh fading coefficients.

Lemma 1. *The overall effective downlink channel matrix of the DFRC MIMO-OFDM system on the n-th symbol subcarrier can be written in frequency domain as [7, 14]*

$$\mathbf{H}_n = \sum_{u=0}^{U-1} \widetilde{\mathbf{H}}_u e^{-\frac{j2\pi u(n-1)}{N_{\rm s}}}, \ \forall n \in \mathcal{N}_{\rm s}. \tag{8}$$

Also, we have $\mathbf{H}_n = [\mathbf{h}_{1,n}^{\rm T}, \cdots, \mathbf{h}_{K,n}^{\rm T}]^{\rm T} \in \mathbb{C}^{K\times N_{\rm t}}$ with $\mathbf{h}_{k,n} = \sum_{u=0}^{U-1} \widetilde{\mathbf{h}}_{k,u} e^{-\frac{j2\pi u(n-1)}{N_{\rm s}}} \in \mathbb{C}^{1\times N_{\rm t}}$. In addition, the received signal of symbol data sequence can be expressed as

$$\mathbf{Y}_{\rm s} = \mathbf{H}_{\rm s}\mathbf{X}_{\rm s} + \mathbf{Z}_{\rm s} \in \mathbb{C}^{N_{\rm s}K\times L} \tag{9}$$

where $\mathbf{H}_{\rm s} = {\rm diag}(\mathbf{H}_1, \cdots, \mathbf{H}_{N_{\rm s}}) \in \mathbb{C}^{N_{\rm s}K\times N_{\rm s}N_{\rm t}}$ and $\mathbf{Z}_{\rm s} \in \mathbb{C}^{N_{\rm s}K\times L}$ is the additive white gaussian noise (AWGN) with i.i.d. random variables following $\mathcal{CN}(0, \sigma^2)$.

2) Multi-user Interference (MUI) and Sum Rate: The downlink MU-MIMO OFDM transmissions will induce MUI, which will have great effects on the performance of the achievable sum rate and the symbol error rate (SER). Assuming that the data symbols for all UEs of $k \in \mathcal{K}$ on all subcarriers of $n \in \mathcal{N}_{\rm s}$ follow the same constellation modulation, we can re-express the compact received signal in (9) as

$$\mathbf{Y}_{\rm s} = \underbrace{\mathbf{S}}_{\rm Signal} + \underbrace{(\mathbf{H}_{\rm s}\mathbf{X}_{\rm s} - \mathbf{S})}_{\rm MUI} + \underbrace{\mathbf{Z}_{\rm s}}_{\rm Noise}, \tag{10}$$

where $\mathbf{H}_{\rm s}\mathbf{X}_{\rm s} - \mathbf{S}$ represents the MUI signals caused by multi-user transmissions [15]. The signal-to-interference-plus-noise ratio (SINR) of UE $k \in \mathcal{K}$ on subcarrier $n \in \mathcal{N}_{\rm s}$ per frame can be further expressed as

$${\rm SINR}_{k,n} = \frac{\mathbb{E}\{|s_{n,k}^l|^2\}}{\mathbb{E}\{|\mathbf{h}_{k,n}\mathbf{x}_{n,l} - s_{n,k}^l|^2\} + \sigma^2}, \tag{11}$$

where $s_{n,k}^l$ is the l-th element of the symbol vector $\mathbf{s}_{n,k}$ and $\mathbf{x}_{n,l} \in \mathbb{C}^{N_{\rm t}\times 1}$ is the l-th column of the precoded symbol matrix $\mathbf{X}_n$ for all UEs. The expectations in (11) are taken with respect to (w.r.t.) the time index $l \in \mathcal{L} = \{1, \cdots, L\}$ [5], and $\mathbb{E}\{|s_{n,k}^l|^2\}$ is fixed with given constellation mode. Hence, the maximum achievable sum rate of the K downlink UEs on subcarrier n can be given as $R_n = \sum_{n=1}^{K} \log_2(1 + {\rm SINR}_{k,n})$, and the average sum rate/spectral efficiency of the MIMO-OFDM system is measured as $R = \frac{1}{N_{\rm s}} \sum_{n=1}^{N_{\rm s}} R_n$.

Note that the MUI is an important performance metric of the DFRC MIMO-OFDM system which should be minimized from the perspective of communications, so as to increase the achievable sum rate and decrease the SER. To this end, in the following we employ the MUI as our objective/cost function for enhancing the communication performance of the DFRC MIMO-OFDM system, given as

$$\min_{\mathbf{X}_{\rm s}} \left\|\mathbf{H}_{\rm s}\mathbf{X}_{\rm s} - \mathbf{S}\right\|_{\rm F}^2. \tag{12}$$

C. MIMO-OFDM Radar Model

1) Radar Beampattern: Radar beampattern is a crucial indicator for measuring the radar detection and tracking performance. Note that designing MIMO radar beampattern can be equivalently transformed into designing the probing signal waveform since the radar beampattern is highly related to the covariance matrix of the probing waveform [5, 16]. For the considered DFRC MIMO-OFDM system, the transmit radar beampattern versus the detection angle θ is written as

$$B_{\rm d}(\theta) = \frac{1}{N_{\rm s}} \sum_{n=1}^{N_{\rm s}} \mathbf{a}^{\rm H}(\theta)\mathbf{R}_{{\rm G},n}\mathbf{a}(\theta), \tag{13}$$

which is averaged on the $N_{\rm s}$ subcarriers. Here $\mathbf{a}(\theta) \in \mathbb{C}^{N_{\rm t}\times 1}$ is the transmit steering vector given as

$$\mathbf{a}(\theta) = \left[e^{-j\frac{N_{\rm t}-1}{2}\pi\sin\theta}, e^{-j\frac{N_{\rm t}-3}{2}\pi\sin\theta}, \cdots, e^{j\frac{N_{\rm t}+1}{2}\pi\sin\theta}\right]^{\rm T}, \quad (14)$$

under the assumption that even number of transmit antennas are equipped at the DFRC-BS ULA and the center of the ULA is chosen as the reference point. In addition, $\mathbf{R}_{{\rm G},n} \in \mathbb{C}^{N_{\rm t}\times N_{\rm t}}$ is the effective spatial covariance matrix of the transmit waveform on the n-th subcarrier for $n \in \mathcal{N}_{\rm s}$ given as $\mathbf{R}_{{\rm G},n} = \frac{1}{L}\mathbf{G}_n\mathbf{G}_n^{\rm H}$. In order to ensure that $\{\mathbf{R}_{{\rm G},n}\}_{n\in\mathcal{N}_{\rm s}}$ are positive-definite, we assume that the frame length satisfies $L \geq N_{\rm t}$, which is easy to achieve in the considered wideband scenario with approximately time-invariant channels.

2) Radar Detection Probability: From the perspective of radar, another important performance indicator is the detection probability. We first express the radar received target echo signal at the l-th snapshot/frame as

$$\mathbf{y}_l^{\rm r} = \alpha\boldsymbol{\Upsilon}(\theta)\mathbf{g}_l^{\rm s} + \mathbf{z}^{\rm r} \in \mathbb{C}^{N_{\rm s}N_{\rm t}\times 1}, \quad (15)$$

which is an expanded radar received echo vector considering the $N_{\rm s}$ i.i.d data streams on the $N_{\rm s}$ subcarriers for $l \in \mathcal{L}$. Here, α is the complex path loss of the radar-target-radar path, $\mathbf{g}_l^{\rm s} = (\mathbf{F}_{\rm s}^{\rm H}\otimes\mathbf{I}_{N_{\rm t}})\mathbf{x}_{{\rm s},l} \in \mathbb{C}^{N_{\rm s}N_{\rm t}\times 1}$ with $\mathbf{x}_{{\rm s},l} \in \mathbb{C}^{N_{\rm s}N_{\rm t}\times 1}$ being the l-th column of the precoded signal matrix $\mathbf{X}_{\rm s}$, and $\mathbf{z}^{\rm r} \sim \mathcal{CN}(0, \sigma_{\rm r}^2\mathbf{I}_{N_{\rm s}N_{\rm t}})$ is the AWGN for radar reception. In addition, $\boldsymbol{\Upsilon}(\theta) = \mathbf{I}_{N_{\rm s}} \otimes \widetilde{\boldsymbol{\Upsilon}}(\theta) \in \mathbb{C}^{N_{\rm s}N_{\rm t}\times N_{\rm s}N_{\rm t}}$ with $\widetilde{\boldsymbol{\Upsilon}}(\theta) = \mathbf{a}_{\rm r}(\theta)\mathbf{a}_{\rm t}^{\rm T}(\theta) \in \mathbb{C}^{N_{\rm t}\times N_{\rm t}}$ where $\mathbf{a}_{\rm r}(\theta)$ and $\mathbf{a}_{\rm t}(\theta)$ are the transmit and receive steering vector with $\mathbf{a}_{\rm r}(\theta) = \mathbf{a}_{\rm t}(\theta) = \mathbf{a}(\theta)$.

Based on the Generalized Likelihood Ratio Test [5, 17], the asymptotic radar detection probability can be written as

$$\mathcal{P}_{\rm D} = 1 - \mathfrak{F}_{\mathcal{X}_2^2(\mu)}(\zeta) = 1 - \mathfrak{F}_{\mathcal{X}_2^2(\mu)}\left(\mathfrak{F}_{\mathcal{X}_2^2}^{-1}(1-\mathcal{P}_{\rm f})\right), \quad (16)$$

where $P_{\rm f} = 1 - \mathfrak{F}_{\mathcal{X}_2^2}(\zeta)$ is the false alarm rate and $\mathfrak{F}_{\mathcal{X}_2^2}$ is the chi-squared cumulative distribution function (CDF) with 2 degrees of freedom (DoFs). In addition, the function $\mathfrak{F}_{\mathcal{X}_2^2(\mu)}$ in (16) is the non-central chi-squared CDF with 2 DoFs and the non-central parameter μ is defined as

$$\begin{aligned}\mu &= L|\alpha|^2 P_{\rm t}^{\rm r}{\rm tr}\left(\boldsymbol{\Upsilon}(\theta)\mathbf{R}_{\rm G}\boldsymbol{\Upsilon}^{\rm H}(\theta)(\sigma_{\rm r}^2\mathbf{I})^{-1}\right)\\ &= {\rm SNR}_{\rm R}{\rm tr}\left(\boldsymbol{\Upsilon}(\theta)\mathbf{R}_{\rm G}\boldsymbol{\Upsilon}^{\rm H}(\theta)\right), \end{aligned} \quad (17)$$

where $P_{\rm t}^{\rm r}$ is the power of the DFRC MIMO-OFDM probing waveform and $\mathbf{R}_{\rm G} = \frac{1}{L}\mathbf{G}\mathbf{G}^{\rm H} \in \mathbb{C}^{N_{\rm s}N_{\rm t}\times N_{\rm s}N_{\rm t}}$. In addition, the signal-to-noise (SNR) ratio of the radar received target echo signal is denoted as ${\rm SNR}_{\rm R} = \frac{L|\alpha|^2 P_{\rm t}}{\sigma_{\rm r}^2}$ [17].

To design our DFRC MIMO-OFDM waveform, we employ a desired benchmark of the MIMO-OFDM radar waveform, denoted as $\mathbf{G}_0 \triangleq (\mathbf{F}_{\rm s}^{\rm H}\otimes\mathbf{I}_{N_{\rm t}})\mathbf{X}_{{\rm s},0}$ with $\mathbf{X}_{{\rm s},0}$ being the radar waveform before IDFT operation, which is capable to achieve desirable detection probability. One such benchmark waveform of $\mathbf{G}_0$ can be obtained by leveraging the *Directional Beampattern Design* [18]. From the viewpoint of radar performance, it is beneficial to make the DFRC waveform $\mathbf{G} = (\mathbf{F}_{\rm s}^{\rm H}\otimes\mathbf{I}_{N_{\rm t}})\mathbf{X}_{\rm s}$ to be as close to $\mathbf{G}_0$ as possible. Hence, the objective/cost function for enhancing the radar performance of the DFRC MIMO-OFDM system is given as

$$\min_{\mathbf{X}_{\rm s}} \left\|(\mathbf{F}_{\rm s}^{\rm H}\otimes\mathbf{I}_{N_{\rm t}})\mathbf{X}_{\rm s} - \mathbf{G}_0\right\|_{\rm F}^2. \quad (18)$$

III. Low-PAPR DFRC Waveform Design

PAPR is defined as the ratio between the maximum power and the average power of the complex passband signal [8], which should be effectively restrained in the practical OFDM systems with low-cost non-linear amplifiers. Based on the results in [8, 12], PAPR levels can be accurately measured if the discrete-time signals are Υ-times interpolated (oversampled) with $\Upsilon \geq 4$. Our aim is to elaborately design the DFRC MIMO-OFDM waveform matrix $\mathbf{X}_{\rm s} \in \mathbb{C}^{N_{\rm s}N_{\rm t}\times L}$ to achieve a desirable performance tradeoff between communications and radar detections under the low-PAPR and power constraints.

A. PAPR of the DFRC MIMO-OFDM Waveform

We first formulate the power allocation constraint on each frame/snapshot $l \in \mathcal{L}$ as

$$\left\|(\dot{\mathbf{F}}^{\rm H}\otimes\mathbf{I}_{N_{\rm t}})\dot{\mathbf{x}}_l\right\|_2^2 = P_{\rm t},\ \forall l \in \mathcal{L}, \quad (19)$$

where $\dot{\mathbf{x}}_l \in \mathbb{C}^{NN_{\rm t}\times 1}$ is the l-th column of $\dot{\mathbf{X}}$ and $P_{\rm t}$ is the transmit power budget for each frame/snapshot. Here, the equality power allocation constraints are leveraged due to the fact that the radar is usually required to transmit at its maximum available power in practice.

Considering an oversampling rate $\Upsilon \geq 4$, the corresponding IDFT of each transmit antenna should with $\Upsilon N_{\rm s}$ input and output points. We further denote $\mathbf{F}_{\rm os} \in \mathbb{C}^{\Upsilon N_{\rm s}\times\Upsilon N_{\rm s}}$ as the normalized oversampling DFT matrix where $F_{i,m}^{\rm os} = \frac{1}{\sqrt{N_{\rm s}}}e^{-j\frac{2\pi}{\Upsilon N_{\rm s}}(i-1)(m-1)}$ is the (i,m)-th element with index $i, m \in \mathcal{N}_{\rm os} = \{1, 2, \cdots, \Upsilon N_{\rm s}\}$. In addition, the precoded symbol matrix should be Υ-times interpolated with 0 as

$$\begin{aligned}\mathbf{X}_{\rm os} = \Big[&\mathbf{X}_1^{\rm T}, \cdots, \mathbf{X}_{N_{\rm s}/2}^{\rm T}, \underbrace{\mathbf{0}, \cdots, \mathbf{0}}_{\Upsilon N_{\rm s}-1\ \mathbf{0}_{L\times N_{\rm t}}},\\ &\mathbf{X}_{N_{\rm s}/2+1}^{\rm T}, \cdots, \mathbf{X}_{N_{\rm s}}^{\rm T}\Big]^{\rm T} \in \mathbb{C}^{\Upsilon N_{\rm s}N_{\rm t}\times L}, \end{aligned} \quad (20)$$

considering even number of subcarriers $N_{\rm s}$, then the oversampled IDFT output can be written as $(\mathbf{F}_{\rm os}^{\rm H}\otimes\mathbf{I}_{N_{\rm t}})\mathbf{X}_{\rm os} \in \mathbb{C}^{\Upsilon N_{\rm s}N_{\rm t}\times L}$. Hence, the PAPR constraint of the oversampled discrete-time signal for the DFRC MIMO-OFDM waveform after IDFT can be expressed as

$$\begin{aligned}{\rm PAPR}(\mathbf{X}_{\rm os}) &= \frac{\max\limits_{\gamma,l}\left|\left[(\mathbf{F}_{\rm os}^{\rm H}\otimes\mathbf{I}_{N_{\rm t}})\mathbf{X}_{\rm os}\right]_{\gamma,l}\right|^2}{\frac{1}{\Upsilon NN_{\rm t}L}\left\|(\dot{\mathbf{F}}_{\rm os}^{\rm H}\otimes\mathbf{I}_{N_{\rm t}})\dot{\mathbf{X}}_{\rm os}\right\|_{\rm F}^2}\\ &\overset{(a)}{=} \frac{\max\limits_{\gamma,l}\left|\left[(\mathbf{F}_{\rm os}^{\rm H}\otimes\mathbf{I}_{N_{\rm t}})\mathbf{X}_{\rm os}\right]_{\gamma,l}\right|^2}{\frac{1}{NN_{\rm t}L}\left\|(\dot{\mathbf{F}}^{\rm H}\otimes\mathbf{I}_{N_{\rm t}})\dot{\mathbf{X}}\right\|_{\rm F}^2}\\ &\overset{(b)}{=} \frac{\max\limits_{\gamma,l}\left|\left[(\mathbf{F}_{\rm os}^{\rm H}\otimes\mathbf{I}_{N_{\rm t}})\mathbf{X}_{\rm os}\right]_{\gamma,l}\right|^2}{\frac{1}{NN_{\rm t}}P_{\rm t}} \leq \varepsilon, \end{aligned} \quad (21)$$

where $\varepsilon \in [1, NN_{\rm t}]$ is indicated as the maximum allowable PAPR threshold of the DFRC MIMO-OFDM system, and $\gamma \in N_{\gamma{\rm st}} \triangleq \{1, \cdots, \Upsilon N_{\rm s}N_{\rm t}\}$, $l \in \mathcal{L}$. In addition,

$$\dot{\mathbf{F}}_{\rm os} = [\mathbf{F}_{\rm os}^{\rm c}, \mathbf{F}_{\rm os}] \in \mathbb{C}^{\Upsilon N_{\rm s}\times(\Upsilon N_{\rm s}+N_{\rm c})}, \quad (22)$$

$$\dot{\mathbf{X}}_{\rm os} = [(\mathbf{X}_{\rm os}^{\rm c})^{\rm T}, \mathbf{X}_{\rm os}^{\rm T}] \in \mathbb{C}^{(\Upsilon N_{\rm s}+N_{\rm c})N_{\rm t}\times L} \quad (23)$$

with $\mathbf{F}_{\rm os}^{\rm c} \in \mathbb{C}^{\Upsilon N_{\rm s}\times N_{\rm c}}$ and $\mathbf{X}_{\rm os}^{\rm c} \in \mathbb{C}^{N_{\rm c}\times N_{\rm t}}$ being formulated by the last $N_{\rm c}$ columns of $\mathbf{F}_{\rm os}$ and the last $N_{\rm c}N_{\rm t}$ rows of

$\mathbf{X}_{\rm os}$, respectively. It is easy to observe that $\mathbf{X}_{\rm os}^{\rm c} = \mathbf{X}_{\rm c}$ in the practical scenario where $N_{\rm c} \leq N_{\rm s}/2$.[2] In (21), (a) and (b) can be easily verified based on the fact that

$$\frac{1}{\Upsilon}\left\|(\dot{\mathbf{F}}_{\rm os}^{\rm H} \otimes \mathbf{I}_{N_{\rm t}})\dot{\mathbf{X}}_{\rm os}\right\|_{\rm F}^2 = \left\|(\dot{\mathbf{F}}^{\rm H} \otimes \mathbf{I}_{N_{\rm t}})\dot{\mathbf{X}}\right\|_{\rm F}^2 = LP_{\rm t}, \quad (24)$$

Hence, the PAPR constraint in (21) is equivalent to the set of PAPR constraints given below:

$$\left|\left[(\mathbf{F}_{\rm os}^{\rm H} \otimes \mathbf{I}_{N_{\rm t}})\mathbf{X}_{\rm os}\right]_{\gamma,l}\right|^2 \leq \frac{\varepsilon P_{\rm t}}{NN_{\rm t}},\ \forall \gamma \in \mathcal{N}_{\gamma{\rm st}},\ \forall l \in \mathcal{L}. \quad (25)$$

It is easy to note the effective elements of the oversampled matrix $\mathbf{X}_{\rm os} \in \mathbb{C}^{\Upsilon N_{\rm s}N_{\rm t} \times L}$ in (20) are exactly the elements of the original precoded symbol matrix $\mathbf{X}_{\rm s} \in \mathbb{C}^{N_{\rm s}N_{\rm t} \times L}$. For utilizing the PAPR constraint (25) and facilitating the formulation of the optimization problem with the effective matrix $\mathbf{X}_{\rm s}$, one challenging lies in transforming $(\mathbf{F}_{\rm os}^{\rm H} \otimes \mathbf{I}_{N_{\rm t}})\mathbf{X}_{\rm os}$ in (25) into a function of $\mathbf{X}_{\rm s}$, which is also a key step for simplifying the problem solving process and reducing the computational complexity. To this end, we further denote an equivalent oversampling DFT matrix $\widetilde{\mathbf{F}}_{\rm os} \in \mathbb{C}^{\Upsilon N_{\rm s} \times N_{\rm s}}$ as

$$\widetilde{\mathbf{F}}_{\rm os} = \begin{cases} \frac{1}{\sqrt{N_{\rm s}}} e^{-j\frac{2\pi}{\Upsilon N_{\rm s}}(n-1)(m-1)}, \\ \qquad n = 1, \cdots, \frac{N_{\rm s}}{2},\ m = 1, \cdots, \Upsilon N_{\rm s}, \\ \frac{1}{\sqrt{N_{\rm s}}} e^{-j\frac{2\pi}{\Upsilon N_{\rm s}}(\Upsilon N_{\rm s} - N_{\rm s} + (n-1))(m-1)}, \\ \qquad n = \frac{N_{\rm s}}{2} + 1 \cdots, N_{\rm s},\ m = 1, \cdots, \Upsilon N_{\rm s}, \end{cases} \quad (26)$$

and it is easy to prove that

$$(\mathbf{F}_{\rm os}^{\rm H} \otimes \mathbf{I}_{N_{\rm t}})\mathbf{X}_{\rm os} = (\widetilde{\mathbf{F}}_{\rm os}^{\rm H} \otimes \mathbf{I}_{N_{\rm t}})\mathbf{X}_{\rm s} \in \mathbb{C}^{\Upsilon N_{\rm s}N_{\rm t} \times L}. \quad (27)$$

Then the PAPR constraints in (25) can be equivalently transformed into

$$\left|\left[(\widetilde{\mathbf{F}}_{\rm os}^{\rm H} \otimes \mathbf{I}_{N_{\rm t}})\mathbf{X}_{\rm s}\right]_{\gamma,l}\right|^2 \leq \frac{\varepsilon P_{\rm t}}{NN_{\rm t}},\ \forall \gamma \in \mathcal{N}_{\gamma{\rm st}},\ \forall l \in \mathcal{L}, \quad (28)$$

which will be used in the following for problem formulation.

B. Problem Formulation

In order to achieve desirable performance tradeoff between communications and radar under the PAPR and power allocation constraints, we can formulate the DFRC MIMO-OFDM waveform optimization problem as

$$\begin{aligned} ({\rm P1}): \min_{\mathbf{X}_{\rm s}}\ & \frac{\rho}{\|\mathbf{S}\|_{\rm F}^2}\left\|\mathbf{H}_{\rm s}\mathbf{X}_{\rm s} - \mathbf{S}\right\|_{\rm F}^2 + \\ & \frac{1-\rho}{\|\mathbf{G}_0\|_{\rm F}^2}\left\|(\mathbf{F}_{\rm s}^{\rm H} \otimes \mathbf{I}_{N_{\rm t}})\mathbf{X}_{\rm s} - \mathbf{G}_0\right\|_{\rm F}^2 \quad (29a) \\ {\rm s.t.}\ & \left|\left[(\widetilde{\mathbf{F}}_{\rm os}^{\rm H} \otimes \mathbf{I}_{N_{\rm t}})\mathbf{X}_{\rm s}\right]_{\gamma,l}\right|^2 \leq \frac{\varepsilon P_{\rm t}}{NN_{\rm t}}, \\ & \forall \gamma \in \mathcal{N}_{\gamma{\rm st}},\ \forall l \in \mathcal{L}, \quad (29b) \\ & \left\|\left(\dot{\mathbf{F}}^{\rm H} \otimes \mathbf{I}_{N_{\rm t}}\right)\dot{\mathbf{x}}_l\right\|_2^2 = P_{\rm t},\ \forall l \in \mathcal{L}, \quad (29c) \end{aligned}$$

where a weighted objective function considering the normalized objectives relating to the performance of communications and radar is leveraged. It is easy to verify that

$$\begin{aligned} & \left\|\left(\dot{\mathbf{F}}^{\rm H} \otimes \mathbf{I}_{N_{\rm t}}\right)\dot{\mathbf{x}}_l\right\|_{\rm F}^2 = \|\dot{\mathbf{g}}_l\|_{\rm F}^2 \\ &= \left\|\left(\mathbf{F}_{\rm s}^{\rm H} \otimes \mathbf{I}_{N_{\rm t}}\right)\mathbf{x}_{{\rm s},l}\right\|_{\rm F}^2 + \left\|\mathbf{\Gamma}_{\rm c}\left(\mathbf{F}_{\rm s}^{\rm H} \otimes \mathbf{I}_{N_{\rm t}}\right)\mathbf{x}_{{\rm s},l}\right\|_{\rm F}^2 \\ &= \|\mathbf{g}_l\|_{\rm F}^2 + \|\mathbf{\Gamma}_{\rm c}\mathbf{g}_l\|_{\rm F}^2 \end{aligned} \quad (30)$$

where $\dot{\mathbf{g}}_l \in \mathbb{C}^{NN_{\rm t}\times 1}$, $\mathbf{x}_{{\rm s},l} \in \mathbb{C}^{N_{\rm s}N_{\rm t}\times 1}$ and $\mathbf{g}_l \in \mathbb{C}^{N_{\rm s}N_{\rm t}\times 1}$ are the l-th column of $\dot{\mathbf{G}}$, $\mathbf{X}_{\rm s}$, and $\mathbf{G}$, respectively. Here, $\mathbf{\Gamma}_{\rm c} \in \mathbb{R}^{N_{\rm s}N_{\rm t}\times N_{\rm s}N_{\rm t}}$ is defined as

$$\mathbf{\Gamma}_{\rm c} = \begin{bmatrix} \mathbf{0}_{(N_{\rm s}-N_{\rm c})N_{\rm t}} & \mathbf{0}_{(N_{\rm s}-N_{\rm c})N_{\rm t}\times N_{\rm c}N_{\rm t}} \\ \mathbf{0}_{N_{\rm c}N_{\rm t}\times(N_{\rm s}-N_{\rm c})N_{\rm t}} & \mathbf{I}_{N_{\rm c}N_{\rm t}} \end{bmatrix} \quad (31)$$

which is utilized to abstract the signals in $\mathbf{G}_l$ used for CP. We further divide the equality power allocation constraint (29c) into two equality power allocation constraints respectively on the symbol signals and the CP signals as

$$\left\|\left(\mathbf{F}_{\rm s}^{\rm H} \otimes \mathbf{I}_{N_{\rm t}}\right)\mathbf{x}_{{\rm s},l}\right\|_{\rm F}^2 = \|\mathbf{g}_l\|_{\rm F}^2 = \beta P_{\rm t}, \quad (32)$$

$$\left\|\mathbf{\Gamma}_{\rm c}\left(\mathbf{F}_{\rm s}^{\rm H} \otimes \mathbf{I}_{N_{\rm t}}\right)\mathbf{x}_{{\rm s},l}\right\|_{\rm F}^2 = \|\mathbf{\Gamma}_{\rm c}\mathbf{g}_l\|_{\rm F}^2 = (1-\beta)P_{\rm t}, \quad (33)$$

by introducing a power splitting parameter $\beta \in (0,1)$. For simplicity, we fix $\beta = \frac{N_{\rm s}}{N}$ and then we have $\beta P_{\rm t} = \frac{N_{\rm s}}{N}P_{\rm t} \triangleq P_{\rm t}^{\rm s}$ and $(1-\beta)P_{\rm t} = \frac{N_{\rm c}}{N}P_{\rm t} \triangleq P_{\rm t}^{\rm c}$, which is reasonable on the basis of average power allocation on data transmissions.[3]

In order to further simplify problem (P1), we denote $\mathbf{D} = \mathbf{F}_{\rm s}^{\rm H} \otimes \mathbf{I}_{N_{\rm t}} \in \mathbb{C}^{N_{\rm s}N_{\rm t}\times N_{\rm s}N_{\rm t}}$ which is a full-rank matrix with

$$\mathbf{D}^{-1} = (\mathbf{F}_{\rm s}^{\rm H})^{-1} \otimes \mathbf{I}_{N_{\rm t}}^{-1} = \mathbf{F}_{\rm s} \otimes \mathbf{I}_{N_{\rm t}} = \mathbf{D}^{\rm H}. \quad (34)$$

Considering $\mathbf{G} = (\mathbf{F}_{\rm s}^{\rm H} \otimes \mathbf{I}_{N_{\rm t}})\mathbf{X}_{\rm s} = \mathbf{D}\mathbf{X}_{\rm s}$, the optimization variable $\mathbf{X}_{\rm s}$ can be re-expressed as $\mathbf{X}_{\rm s} = \mathbf{D}^{-1}\mathbf{G}$. Let $\mathbf{H}_{\rm D} = \mathbf{H}_{\rm s}\mathbf{D}^{-1} \in \mathbb{C}^{N_{\rm s}K\times N_{\rm s}N_{\rm t}}$, then problem (P1) in (29) with power allocation constraints (32), (33) can be further rewritten as

$$\begin{aligned} ({\rm P2}): \min_{\mathbf{G}}\ & \frac{\rho}{\|\mathbf{S}\|_{\rm F}^2}\left\|\mathbf{H}_{\rm D}\mathbf{G} - \mathbf{S}\right\|_{\rm F}^2 + \frac{1-\rho}{\|\mathbf{G}_0\|_{\rm F}^2}\left\|\mathbf{G} - \mathbf{G}_0\right\|_{\rm F}^2 \quad (35a) \\ {\rm s.t.}\ & \left|[\mathbf{\Theta}\mathbf{G}]_{\gamma,l}\right|^2 \leq \frac{\varepsilon P_{\rm t}}{NN_{\rm t}},\ \forall \gamma \in \mathcal{N}_{\gamma{\rm st}},\ \forall l \in \mathcal{L}, \quad (35b) \\ & \|\mathbf{g}_l\|_{\rm F}^2 = P_{\rm t}^{\rm s},\ \forall l \in \mathcal{L}, \quad (35c) \\ & \|\mathbf{\Gamma}_{\rm c}\mathbf{g}_l\|_{\rm F}^2 = P_{\rm t}^{\rm c},\ \forall l \in \mathcal{L}, \quad (35d) \end{aligned}$$

where $\mathbf{\Theta} = \mathbf{D}_{\rm os}\mathbf{D}^{-1} \in \mathbb{C}^{\Upsilon N_{\rm s}N_{\rm t}\times N_{\rm s}N_{\rm t}}$ with $\mathbf{D}_{\rm os} = \widetilde{\mathbf{F}}_{\rm os}^{\rm H} \otimes \mathbf{I}_{N_{\rm t}}$. The problem (P2) in (35) can be solved by directly optimizing $\mathbf{G} \triangleq (\mathbf{F}_{\rm s}^{\rm H} \otimes \mathbf{I}_{N_{\rm t}})\mathbf{X}_{\rm s}$, and we can further simplify the problem-solving process through the following Lemma.

Lemma 2. *Problem (P2) in* (35) *can be optimally solved by addressing L sub-problems parallelly as follows*

$$\begin{aligned} ({\rm P3}): \min_{\{\mathbf{g}_l\}}\ & \frac{\rho}{\|\mathbf{S}\|_{\rm F}^2}\left\|\mathbf{H}_{\rm D}\mathbf{g}_l - \mathbf{s}_l\right\|^2 + \frac{1-\rho}{\|\mathbf{G}_0\|_{\rm F}^2}\left\|\mathbf{g}_l - \mathbf{g}_{0,l}\right\|^2 \quad (36a) \\ {\rm s.t.}\ & {\rm diag}(\mathbf{\Theta}\mathbf{g}_l\mathbf{g}_l^{\rm H}\mathbf{\Theta}^{\rm H}) \leq \frac{\varepsilon P_{\rm t}}{NN_{\rm t}}\mathbf{1}_{\Upsilon N_{\rm s}N_{\rm t}}, \quad (36b) \\ & \|\mathbf{g}_l\|^2 = P_{\rm t}^{\rm s}, \quad (36c) \\ & \|\mathbf{\Gamma}_{\rm c}\mathbf{g}_l\|^2 = P_{\rm t}^{\rm c}, \quad (36d) \end{aligned}$$

which corresponds to the frame/snapshot $l \in \mathcal{L}$.

Lemma 2 provides a low-complexity method for solving the problem (P2) in (35). Next, we will focus on solving the sub-problem (P3) in (36) for $l \in \mathcal{L}$.

[2] In order to improve the energy efficiency of practical OFDM communication systems, the number of symbols is usually set to be much larger than the length of CP, i.e., $N_{\rm s} \gg N_{\rm c}$. In the scenario considered in this paper, we assume that $N_{\rm s}/2 \geq N_{\rm c}$.

[3] The technique of CP is beneficial to avoid ISI cased by frequency-selective fading but at the cost of consuming extra energy and thus degrade the energy efficiency. The effects of adding CP on the degradation of energy efficiency can be eliminated by enlarging $N_{\rm s}$ where $\beta = \frac{N_{\rm s}}{N}$ can approach to 1.

C. MIMO-OFDM DFRC Waveform Design

It is easy to verify that the objective function of problem (P3) in (36) can be equivalently re-expressed in the form of

$$\left\|\mathbf{A}\mathbf{g}_l - \mathbf{b}_l\right\|_{\mathrm{F}}^2 \tag{37}$$

where $\mathbf{A} = \left[\frac{\sqrt{\rho}}{\|\mathbf{S}\|_{\mathrm{F}}}\mathbf{H}_{\mathrm{D}}^{\mathrm{T}}, \frac{\sqrt{1-\rho}}{\|\mathbf{G}_0\|_{\mathrm{F}}}\mathbf{I}_{N_{\mathrm{s}}N_{\mathrm{t}}}\right]^{\mathrm{T}} \in \mathbb{C}^{(N_{\mathrm{s}}K+N_{\mathrm{s}}N_{\mathrm{t}})\times N_{\mathrm{s}}N_{\mathrm{t}}}$ and $\mathbf{b}_l = \left[\frac{\sqrt{\rho}}{\|\mathbf{S}\|_{\mathrm{F}}}\mathbf{s}_l^{\mathrm{T}}, \frac{\sqrt{1-\rho}}{\|\mathbf{G}_0\|_{\mathrm{F}}}\mathbf{g}_{0,l}^{\mathrm{T}}\right]^{\mathrm{T}} \in \mathbb{C}^{(N_{\mathrm{s}}K+N_{\mathrm{s}}N_{\mathrm{t}})\times 1}$. Moreover, the minimization of the objective function in (37) without any constraints can be equivalently transformed into a problem with an auxiliary parameter ξ as follows

$$\min_{\mathbf{g}_l} \left\|\mathbf{A}\mathbf{g}_l - \xi\mathbf{b}_l\right\|^2, \quad \text{s.t. } |\xi|^2 = 1. \tag{38}$$

Based on this observation, problem (P3) in (36) can be equivalently reformulated as ‘

$$(\mathrm{P4}): \min_{\mathbf{g}_l,\xi} \quad [\mathbf{g}_l^{\mathrm{H}}, \xi^*]\begin{bmatrix}\mathbf{A}^{\mathrm{H}}\mathbf{A} & -\mathbf{A}^{\mathrm{H}}\mathbf{b}_l \\ -\mathbf{b}_l^{\mathrm{H}}\mathbf{A} & \mathbf{b}_l^{\mathrm{H}}\mathbf{b}_l\end{bmatrix}\begin{bmatrix}\mathbf{g}_l \\ \xi\end{bmatrix} \tag{39a}$$

$$\text{s.t.} \quad \mathrm{diag}(\mathbf{\Theta}\mathbf{g}_l\mathbf{g}_l^{\mathrm{H}}\mathbf{\Theta}^{\mathrm{H}}) \le \frac{\varepsilon P_{\mathrm{t}}}{NN_{\mathrm{t}}}\mathbf{1}_{\Upsilon N_{\mathrm{s}}N_{\mathrm{t}}}, \tag{39b}$$

$$\|\mathbf{g}_l\|^2 = LP_{\mathrm{t}}^{\mathrm{s}}, \tag{39c}$$

$$\left\|\widetilde{\mathbf{\Gamma}}_{\mathrm{c}}\mathbf{g}_l\right\|^2 = LP_{\mathrm{t}}^{\mathrm{c}}, \tag{39d}$$

$$|\xi|^2 = 1, \tag{39e}$$

which is a homogeneous quadratically constrained quadratic program (QCQP) and can be solved by SDR. We denote

$$\widehat{\mathbf{g}} = [\mathbf{g}_l^{\mathrm{H}}, \xi^*]^{\mathrm{H}} \in \mathbb{C}^{(N_{\mathrm{s}}N_{\mathrm{t}}+1)\times 1}, \tag{40}$$

$$\widehat{\mathbf{G}} = \widehat{\mathbf{g}}_l\widehat{\mathbf{g}}_l^{\mathrm{H}} \in \mathbb{C}^{(N_{\mathrm{s}}N_{\mathrm{t}}+1)\times(N_{\mathrm{s}}N_{\mathrm{t}}+1)}, \tag{41}$$

$$\mathbf{Q} = \begin{bmatrix}\mathbf{A}^{\mathrm{H}}\mathbf{A} & -\mathbf{A}^{\mathrm{H}}\mathbf{b}_l \\ -\mathbf{b}_l^{\mathrm{H}}\mathbf{A} & \mathbf{b}_l^{\mathrm{H}}\mathbf{b}_l\end{bmatrix} \in \mathbb{C}^{(N_{\mathrm{s}}N_{\mathrm{t}}+1)\times(N_{\mathrm{s}}N_{\mathrm{t}}+1)}, \tag{42}$$

$$\widehat{\mathbf{\Gamma}}_{\mathrm{c}} = \begin{bmatrix}\mathbf{\Gamma}_{\mathrm{c}}^{\mathrm{H}}\mathbf{\Gamma}_{\mathrm{c}} & \mathbf{0}_{N_{\mathrm{s}}N_{\mathrm{t}}\times 1} \\ \mathbf{0}_{1\times N_{\mathrm{s}}N_{\mathrm{t}}} & 0\end{bmatrix} \in \mathbb{C}^{(N_{\mathrm{s}}N_{\mathrm{t}}+1)\times(N_{\mathrm{s}}N_{\mathrm{t}}+1)}, \tag{43}$$

problem (P4) in (39) can be further rewritten as

$$(\mathrm{P5}): \min_{\widehat{\mathbf{G}}} \quad \mathrm{Tr}(\mathbf{Q}\widehat{\mathbf{G}}) \tag{44a}$$

$$\text{s.t.} \quad \mathrm{diag}(\widehat{\mathbf{\Theta}}\widehat{\mathbf{G}}\widehat{\mathbf{\Theta}}^{\mathrm{H}}) \le \frac{\varepsilon P_{\mathrm{t}}}{NN_{\mathrm{t}}}\mathbf{1}_{\Upsilon N_{\mathrm{s}}N_{\mathrm{t}}}, \tag{44b}$$

$$\mathrm{Tr}(\widehat{\mathbf{G}}) = P_{\mathrm{t}}^{\mathrm{s}} + 1, \tag{44c}$$

$$\mathrm{Tr}(\widehat{\mathbf{\Gamma}}_{\mathrm{c}}\widehat{\mathbf{G}}) = P_{\mathrm{t}}^{\mathrm{c}}, \tag{44d}$$

$$\widehat{\mathbf{G}}_{N_{\mathrm{s}}N_{\mathrm{t}}+1,N_{\mathrm{s}}N_{\mathrm{t}}+1} = 1, \tag{44e}$$

$$\widehat{\mathbf{G}} \succeq \mathbf{0}, \tag{44f}$$

$$\mathrm{rank}(\widehat{\mathbf{G}}) = 1, \tag{44g}$$

through optimizing the hermitian semi-definite matrix variable $\widehat{\mathbf{G}}$ where $\widehat{\mathbf{\Theta}} = \left[\mathbf{\Theta}\ \mathbf{0}_{\Upsilon N_{\mathrm{s}}N_{\mathrm{t}}\times 1}\right] \in \mathbb{C}^{\Upsilon N_{\mathrm{s}}N_{\mathrm{t}}\times(N_{\mathrm{s}}N_{\mathrm{t}}+1)}$. By dropping the rank-1 constraint (44g), problem (P5) becomes a standard SDP and can be effectively solved by the classic SDR technique via the existing numerical tools, e.g., CVX.

Lemma 3. *It can be proved that the rank-1 solution exist in general for the SDR of problem (P5) in* (44)*, indicating that the globally optimal solution of problem (P5) can always be obtained by solving its SDR without considering the rank-1 constraint* (44g)*, denoted as* $\widehat{\mathbf{G}}^{\mathrm{o}}$ *[18].*

IV. Simulation Results

In this section, simulation results are given to demonstrate the effectiveness of the proposed methods for designing the low-PAPR DFRC MIMO-OFDM waveform. The basic simulation parameters are listed in Table I unless specified otherwise. The obtained results in the following figures are averaged over 1000 Monte Carlo simulations.

TABLE I
Simulation Parameters

Parameter	Symbol	Value
Number of transmit antennas at the DFRC-BS	N_{t}	8
Number of subcarriers	N_{s}	16
Number of non-zero channel taps	U	4
Length of CP	N_{c}	3
Number of active UEs	K	2
Number of targets	M	3
The frame length	L	128
Power budget for each OFDM symbol	P_{t}	1W
Oversampling rate	Υ	4

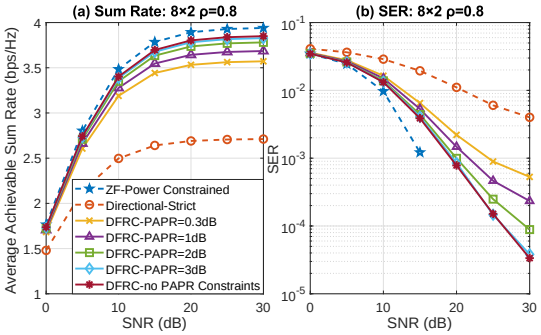

Fig. 1. The average achievable sum rate and SER versus SNR.

1) Performance for Communications: In Fig. 2, the communication performance of average sum rate and SER versus SNR are shown in scenario of communication priority with $\rho = 0.8$. It is easy to observe that the communication-only ZF-Power Constrained scheme provides a upper bound while the radar-only Directional-Strict scheme provides a lower bound for communication performance. The sum rate and SER for the proposed DFRC scheme is highly superior to the Directional-Strict scheme and close to the ZF-Power Constrained scheme. The average sum rates of all the schemes gradually saturate as SNR increases due to the fact the noise power gradually becomes negligible considering the fixed limited signal power and thus MUI dominates.

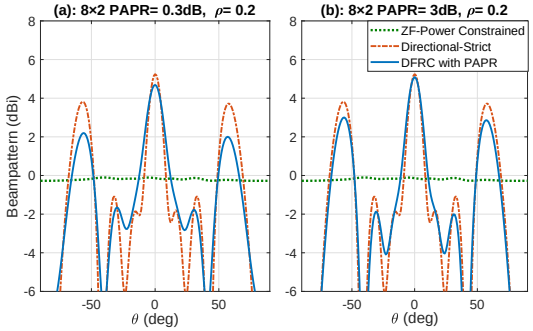

Fig. 2. Radar beampatterns of the waveform versus angles.

2) Performance for Radar: In Fig. 3, the radar performance of detection beampattern are presented in the scenario of radar

priority with $\rho = 0.2$, where three targets of interest with angles of $-\pi/3$, 0 and $\pi/3$ are considered. It demonstrates the effectiveness of the designed low-PAPR DFRC MIMO-OFDM waveform in detecting targets. The beampattern of the proposed DFRC scheme can well match the desired Directional-Strict scheme and can be enhanced by relaxed PAPR constraints. For the communication-only ZF-Power Constrained scheme, the beam gains at all directions are almost the same which is impossible to detect the interested targets.

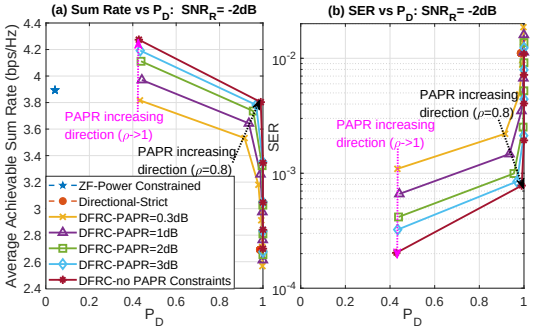

Fig. 3. The average achievable communication sum rate and SER for SER=20dB versus the radar detection probability $\mathcal{P}_{\mathrm{D}}$ for $\mathrm{SNR}_{\mathrm{R}}$=−2dB.

3) Performance Tradeoff: In this section, we try to analyze the direct performance tradeoff between functionalities of communications and radar. The communication results of average sum rate and SER versus the radar detection probability $\mathcal{P}_{\mathrm{D}}$ are depicted in Fig. 4 for $\mathrm{SNR}_{\mathrm{R}} = -2\mathrm{dB}$. The six points shown in this figures correspond to $\rho = [0.01, 0.2, 0.4, 0.6, 0.8, 0.99]$. We can observe that the $\mathcal{P}_{\mathrm{D}}$ requirements are easier to be satisfied since most of the points are located in the area of $\mathcal{P}_{\mathrm{D}} \geq 0.8$, and thus the satisfactory settings of ρ and PAPR thresholds can be flexibly selected based on the requirements of sum rate and SER.

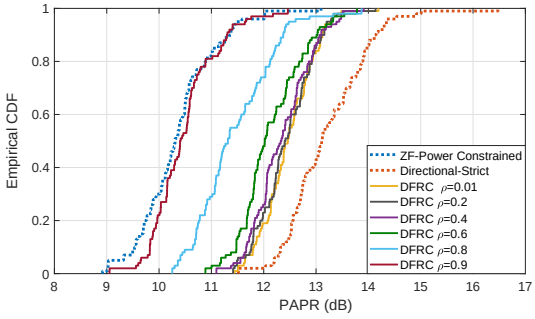

Fig. 4. The empirical CDF of the PAPR (dB).

In Fig. 5, the empirical CDFs of waveform PAPR for the proposed DFRC scheme and the two benchmarks are provided, where the PAPR constraints are not considered. It is clear to see that the PAPR of the DFRC scheme is within the range of [9,14]dB which are too high to satisfy the strict hardware requirements. In comparison with the previous simulation results, we can clearly observe that we can restrain the PAPR levels of the DFRC waveform to 3dB, 2dB, 1dB and even 0.3dB without too much performance degradation for both communications and radar, demonstrating the feasibility and effectiveness of the proposed low-PAPR DFRC MIMO-OFDM waveform design method.

V. Conclusion

In this paper, the low-PAPR DFRC MIMO-OFDM waveform design is investigated. A weighted objective function on normalized communication and radar performance metrics is minimized under the transmit power and PAPR constraints. The optimization problem can be equivalently solved by addressing sub-problem parallelly, and each sub-problem can be optimally solved by the SDR method satisfying the rank-1 constraint. The simulation results are provided to verify the feasibility, effectiveness, and flexibility of the proposed low-PAPR DFRC MIMO-OFDM waveform design method.

Acknowledgment

This work is supported by the U.K. EPSRC under grant EP/S028455/1.

References

[1] A. Hassanien, M. G. Amin, E. Aboutanios, and B. Himed, "Dual-function radar communication systems: A solution to the spectrum congestion problem," *IEEE Signal Process. Mag.*, vol. 36, no. 5, pp. 115–126, 2019.

[2] D. Ma, N. Shlezinger, T. Huang, Y. Liu, and Y. C. Eldar, "Joint radar-communication strategies for autonomous vehicles: Combining two key automotive technologies," *IEEE Signal Process. Mag.*, vol. 37, no. 4, pp. 85–97, 2020.

[3] F. Liu, C. Masouros, A. P. Petropulu, H. Griffiths, and L. Hanzo, "Joint radar and communication design: Applications, state-of-the-art, and the road ahead," *IEEE Trans. Commun.*, vol. 68, no. 6, pp. 3834–3862, 2020.

[4] J. A. Zhang, F. Liu, C. Masouros, R. W. Heath Jr, Z. Feng, L. Zheng, and A. Petropulu, "An overview of signal processing techniques for joint communication and radar sensing," *arXiv preprint arXiv:2102.12780*, 2021.

[5] F. Liu, L. Zhou, C. Masouros, A. Li, W. Luo, and A. Petropulu, "Toward dual-functional radar-communication systems: Optimal waveform design," *IEEE Trans. Signal Process.*, vol. 66, no. 16, pp. 4264–4279, 2018.

[6] X. Liu, T. Huang, N. Shlezinger, Y. Liu, J. Zhou, and Y. C. Eldar, "Joint transmit beamforming for multiuser MIMO communications and mimo radar," *IEEE Trans. Signal Process.*, vol. 68, pp. 3929–3944, 2020.

[7] D. Tse and P. Viswanath, *Fundamentals of wireless communication*. Cambridge university press, 2005.

[8] Y. S. Cho, J. Kim, W. Y. Yang, and C. G. Kang, *MIMO-OFDM wireless communications with MATLAB*. John Wiley & Sons, 2010.

[9] C. Shi, Y. Wang, F. Wang, S. Salous, and J. Zhou, "Joint optimization scheme for subcarrier selection and power allocation in multicarrier dual-function radar-communication system," *IEEE Syst. J.*, vol. 15, no. 1, pp. 947–958, 2021.

[10] T. Tian, T. Zhang, L. Kong, and Y. Deng, "Transmit/receive beamforming for MIMO-OFDM based dual-function radar and communication," *IEEE Trans. Veh. Technol.*, vol. 70, no. 5, pp. 4693–4708, 2021.

[11] M. F. Keskin, V. Koivunen, and H. Wymeersch, "Limited feedforward waveform design for OFDM dual-functional radar-communications," *IEEE Trans. Signal Process.*, vol. 69, pp. 2955–2970, 2021.

[12] S. H. Han and J. H. Lee, "An overview of peak-to-average power ratio reduction techniques for multicarrier transmission," *IEEE Wireless Commun.*, vol. 12, no. 2, pp. 56–65, 2005.

[13] G. Wunder, R. F. Fischer, H. Boche, S. Litsyn, and J.-S. No, "The PAPR problem in OFDM transmission: New directions for a long-lasting problem," *IEEE Signal Process. Mag.*, vol. 30, no. 6, pp. 130–144, 2013.

[14] B. Muquet, Z. Wang, G. Giannakis, M. de Courville, and P. Duhamel, "Cyclic prefixing or zero padding for wireless multicarrier transmissions?" *IEEE Trans. Commun.*, vol. 50, no. 12, pp. 2136–2148, 2002.

[15] S. K. Mohammed and E. G. Larsson, "Per-antenna constant envelope precoding for large multi-user MIMO systems," *IEEE Trans. Commun.*, vol. 61, no. 3, pp. 1059–1071, 2013.

[16] J. Li and P. Stoica, *MIMO radar signal processing*. John Wiley & Sons, 2008.

[17] I. Bekkerman and J. Tabrikian, "Target detection and localization using MIMO radars and sonars," *IEEE Trans. Signal Process.*, vol. 54, no. 10, pp. 3873–3883, 2006.

[18] X. Hu, C. Masouros, F. Liu, and R. Nissel, "MIMO-OFDM dual-functional radar-communication systems: Low-PAPR waveform design," *arXiv preprint arXiv:2109.13148*, 2021.